

DOI: https://doi.org/10.30898/1684-1719.2025.11.21

17th International Conference

Gas Discharge Plasmas and Their Applications

Ekaterinburg, Russia, 8-12 September 2025

FEATURES OF THE FORMATION OF A HIGH-VOLTAGE NANOSECOND DISCHARGE IN A "POINT-TO-POINT" GAP FILLED WITH ATMOSPHERIC-PRESSURE AIR

D.V. Beloplotov ¹, B. Zaitsev ², D.A. Sorokin ^{1,2}

¹ Institute of High Current Electronics SB RAS,
 634055, Russia, Tomsk, 2/3 Akademichesky Ave.
 ² National Research Tomsk State University,
 634050, Russia, Tomsk, 36 Lenina Ave.

The paper was received October 2, 2025.

Abstract. Using high-speed scientific equipment, studies of high-voltage nanosecond discharge in a gap with two pointed electrodes filled with atmospheric-pressure air were carried out. The physical processes occurring during the discharge formation and combustion were studied using optical imaging and oscillography techniques. A stage-by-stage description of the phenomenon evolution obtained with high spatio-temporal resolution is presented. The fact of a collision of streamers propagating towards each other, occurring at a distance of $\sim 2/3$ of the interelectrode distance and accompanied by an increase in the intensity of the plasma glow and the electric field strength at the meeting point, has been experimentally recorded.

Keywords: high-voltage nanosecond discharge, "point-to-point" gap, streamer, diffuse discharge, spark, nonuniform electric field, atmospheric pressure air.

Funding: The studies were performed in the framework of the State Task for IHCE SB RAS, project # FWRM-2021-0014.

Corresponding author: Dmitry Alekseevich Sorokin, SDmA-70@loi.hcei.tsc.ru

Introduction

A high-voltage nanosecond discharge in a gas-filled gap with a strongly non-uniform electric field strength distribution has attracted the attention of researchers around the world for many years [1–14]. This circumstance is explained by the unique features inherent in this phenomenon, which give it the potential to be used as a basis for technical solutions and technological processes (see, e.g., [1, 4, 15–17] and references in them).

For example, it is known that the ignition of this type of discharge is characterized by an ultra-short (hundreds of picoseconds) breakdown phase, before the completion of which a large (hundreds of amperes) current flows in the external circuit [18–20]. This makes it possible to use the high-voltage nanosecond discharge in the creation of a new type of switching devices for solving problems in the field of high-current electronics.

On the other hand, this discharge is a way of obtaining dense, non-equilibrium, low-temperature plasma in gaseous, over a wide range of pressures, and liquid media [4, 17, 21–23]. Such plasma contains energetic electrons and photons, ionized and excited particles, and a wide range of chemically active species [21, 24–26]. The described plasma object is an attractive tool for advanced plasma technologies with high potential for use in a wide variety of fields, such as science, lighting engineering, industrial pollution control, material processing, transport technology, agriculture, medicine, etc. [17, 21, 27–31].

In this context, the high-voltage nanosecond discharge in atmospheric air is especially preferable. This is due to the rich initial composition of the plasma-forming medium, combined with the absence of the need to use expensive equipment to maintain a gas mixture pressure different from atmospheric. Although research into the phenomenon under consideration is being conducted quite actively, the path from a

laboratory setup to full-fledged industrial implementation in various directions is still far from the finish line.

This is explained, in large part, by the fact that the designated object is a multifaceted phenomenon, the study of which is associated with a number of challenges for the researcher. The formation of the high-voltage nanosecond discharge in a gas-phase medium occurs, as a rule, in an interelectrode gap, containing at least one element with a small radius of curvature (needle, blade, tube, ball), providing a non-uniform distribution of the electric field strength and, as a consequence, overvoltage of tens to hundreds of percent [8, 20]. A high-voltage voltage pulse with a high rate of increase to the amplitude value is applied to the electrode with a small radius of curvature. This initiates the process of streamer (an ionization wave) development, which ensures the increase in conductivity in the gap and its breakdown, followed by discharge combustion in a diffuse form [4]. This form of discharge combustion is characterized by the formation of a non-equilibrium low-temperature plasma, the properties of which are determined by the kind and pressure of the plasma-forming medium, excitation parameters and the diode design.

The concept, which is understandable in general terms, is complicated by the fact that when the phenomenon is implemented, a series of physical processes that determine the result take place, depending on the initial conditions and occurring on extremely small spatial-temporal scales. This, of course, imposes certain requirements on the methods and equipment for studying the phenomenon.

Most often, a "point-to-plane" gap is chosen for the implementation of the high-voltage nanosecond discharge, since in this case the plasma formation has the shape of a diverging cone and is of interest from the point of view of the impact on various objects, since it provides the largest contact area with the target electrode [4, 14].

When it is necessary to localize the plasma, for example, when implementing a point source of radiation or a switching device, the most preferable option is the "point-to-point" geometry [2]. In this case, it is assumed that the breakdown should occur due to the development of oppositely directed streamers from each of the electrodes. During the the breakdown, these streamers must collide, forming a region of enhanced

electric field, which is a source of electromagnetic radiation, in particular, X-rays [32]. However, due to the fact that the breakdown of air at atmospheric pressure under such conditions occurs in fractions of nanoseconds, when studying the fundamental aspects of high-voltage nanosecond discharge in this case, it is necessary to use advanced scientific equipment.

It should be noted that in [33], when igniting a high-voltage nanosecond discharge in water in order to study the possibility of cleaning it from organic contaminants, due to the sufficiently high density of the plasma-forming medium, it was possible to visualize the process of breakdown development and subsequent combustion of the discharge. In this case, in the images of the plasma channel glow obtained by shooting with a digital camera and an ICCD camera equipped with a long-focus lens, an area in the gap that differed from the neighboring areas by a more intense glow was observed. It was suggested that this region was a meeting place of oppositely propagating streamers.

The aim of this paper is to study various aspects of the formation and combustion of the high-voltage nanosecond discharge in a "point-to-point" gap filled with atmospheric pressure air.

1. Experimental setup and techniques

The studies were carried out on an experimental setup presented in fig. 1.

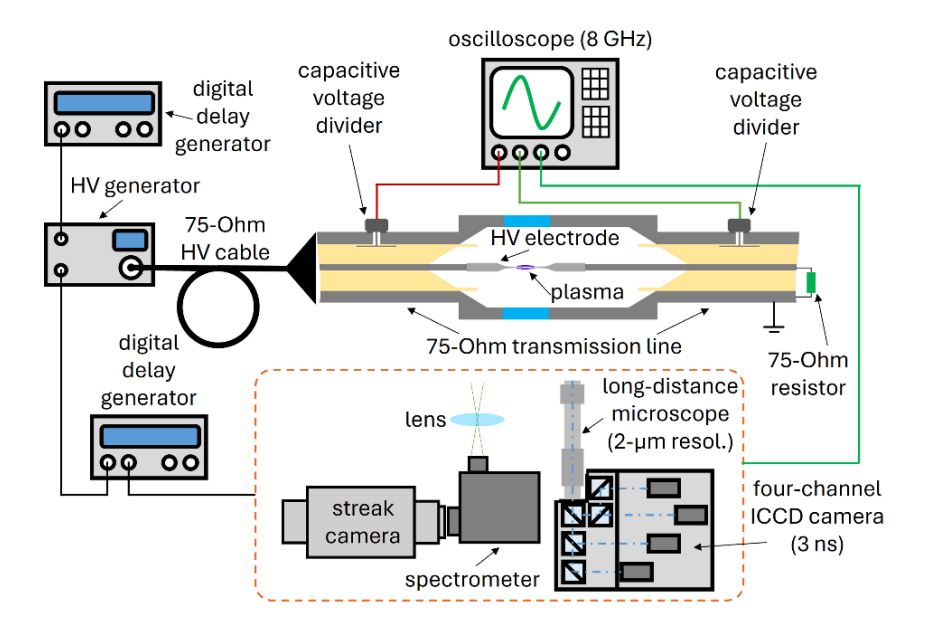


Fig. 1. Sketch of the experimental setup.

The basis of the setup was a coaxial discharge chamber with high-voltage transmission lines (wave resistance is 75 Ohm), equipped with capacitive voltage dividers (CVD). There was an interelectrode assembly inside the chamber in a break of the central high-voltage conductor. The assembly was formed by two stainless steel sewing needles with a radius of curvature of the tip part of 75 μ m. The needles were mounted on metal cylinders with a diameter of 6 mm, which were installed on two opposite parts of the conductor break. The interelectrode distance was 4 mm.

There were quartz windows (KU-1 grade) on the sides of the discharge chamber. The windows provided the possibility of visual observation and the output of optical radiation from the discharge plasma. In the experiments, the chamber was filled with air at a pressure of 760 Torr.

To initiate the discharge, voltage pulses from a GIN-50-01 generator (FID GmbH, Burbach, Germany, [34]) were applied to the gap. The generator was connected to the transmission line via a 3-m-length cable with the wave resistance of 75 Ohm. The discharge was ignited in a single mode by voltage pulses of positive polarity with an amplitude value of \approx +25 kV, a rise and fall time of \approx 2.2 ns, and a half-height duration of \approx 13 ns. The energy stored in the incident voltage wave was \approx 100 mJ (at +25 kV).

The other end of the transmission line was connected to a 75-Ohm TVO resistor. This element absorbed the voltage pulse that passed through the discharge gap into the second line.

CVDs before and after the discharge gap recorded voltage pulses: incident, reflected from the gap and passed through it. Using these data, the voltage across the gap and the current through it were determined.

Time-integrated images of discharge plasma glow were obtained with a Canon EOS R full-frame digital mirrorless camera (Canon Ltd., Japan) with a resolution and size of matrix, respectively, 30.3 megapixels and 36×24 mm². The digital camera was equipped with a K2 Distamax (Infinity Photo-Optical Company, USA) long-focus microscope with a CF-3 objective providing an optical resolution of up to 1.7 μm.

Time-resolved images of discharge plasma glow were obtained with a four-channel HSFC-PRO (PCO Computer Optics GmbH, Germany) ICCD camera. The ICCD camera provided capturing of four consecutive frames with a minimum exposure of 3 ns each and an adjustable delay between them (up to ≈ 0.1 ns). The spectral sensitivity range of each channel of the ICCD camera lies in the wavelength range of 200–900 nm. The K2 Distamax long-focus microscope was also used as an objective. Synchronization of the ICCD camera and the high-voltage generator was provided by a DG645 (Stanford Research Systems, USA) digital delay generator.

The spatiotemporal dynamics of the magnitude of the reduced electric field strength E/N [Td = 10^{-21} V·m²] (E is the electric field strength [V], N is the concentration of the plasma-forming gas [m-3]) was also determined at the breakdown development stage, including for the purpose of identifying the fact of streamer collision. The E/N value was measured using the optical emission spectroscopy (OES) method based on the radiation-collision model of plasma. The plasma of high-voltage nanosecond discharge fully complies with this model. The method involves determining the ratio $R_{391/394}$ of the intensities of bands with wavelengths $\lambda = 391.4$ and $\lambda = 394.3$ nm, formed, respectively, by the spectral transitions of the first negative (1^{-}) and second positive (2^{+}) systems of a molecular ion N_2^{+} and a nitrogen molecule N₂, using which the value of the reduced electric field strength is calculated [35, 36]. The value of $R_{391/394}$ was determined based on the recorded time behavior of the intensity of the spectral bands using an ultra-high-speed complex consisting of a Hamamatsu C10910-05 streak camera (Hamamatsu Photonics K.K., Japan) equipped with an Acton SP2300 spectrometer (Princeton Instruments Inc., USA) with a diffraction grating of 1200 grooves/mm. Using the experimentally measured ratio $R_{391/394}$ and the empirical expression (1), where N_0 is the gas concentration under normal conditions, the value of E/N (or E) can be obtained in the region of the interelectrode gap and the time moment of interest to us.

$$R_{391/394}\left(\frac{E}{N}, N_0\right) = e^{-89\cdot\left(\frac{E}{N}\right)^{-\frac{1}{2}}}.$$
 (1)

The streak camera and high-voltage generator were also synchronized using the DG645 digital delay generator. In each region of the interelectrode gap of interest, 1000 time-resolved patterns of the spectral distribution of radiation intensity were recorded. Then, the noise of the CCD matrix of a Hamamatsu ORCA-R2 C10600-10B (Hamamatsu Photonics K.K., Japan) of the streak camera, recorded separately, was averaged and subtracted.

An MSO64B digital real-time oscilloscope (Tektronix Inc., USA) with a bandwidth of 8 GHz and a sampling rate of up to 50 GS/s was used for simultaneous recording of electrical signals from CVDs and trigger signals of the measuring equipment. The signals from the probes were transported via RG58-A/U radio frequency cables (Radiolab Ltd., Antenna Network Lab. Inc., USA), attenuated, if necessary, by 142-NM attenuators (Barth Electronics Inc., USA).

2. Results and discussion

As noted in the Introduction, a number of experiments have been conducted to investigate various aspects of the HV nanosecond discharge in a "point-to-point" gap filled with atmospheric pressure air.

When a quasi-rectangular HV pulse is applied across the gap, two discharge modes are implemented depending on the pulse energy: a diffuse discharge – with a pulse energy of 1.2 mJ, and the diffuse discharge with a subsequent transition to a spark – with a pulse energy of 103 mJ.

Fig. 2 shows time-integrated images of the discharge plasma glow in atmospheric-pressure air between two needle electrodes for different voltage pulse energies.

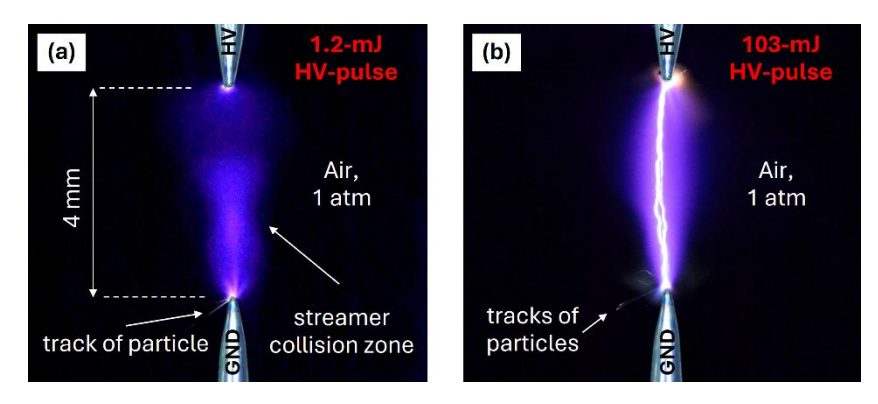


Fig. 2. Time-integrated images of the discharge plasma glow between two needle electrodes. Air, 760 Torr. Different energy reserve in HV pulses. HV – high-voltage electrode, GND –opposite electrode shunted through a 75-Ohm resistor.

As can be seen from fig. 2a, the diffuse discharge is characterized by a quasi-uniform plasma glow in the interelectrode gap with local areas of increased intensity near the electrodes. At the distance of $\sim 1/4$ of the gap length from the HV electrode, a zone of reduced brightness is observed. There, as will be shown below, a streamer reaches its largest diameter. At the distance of $\sim 2/3$ of the gap length from the HV electrode, a narrow bright region is observed. It is associated with the interaction of oppositely directed streamers. A detailed analysis of the discharge evolution is presented below.

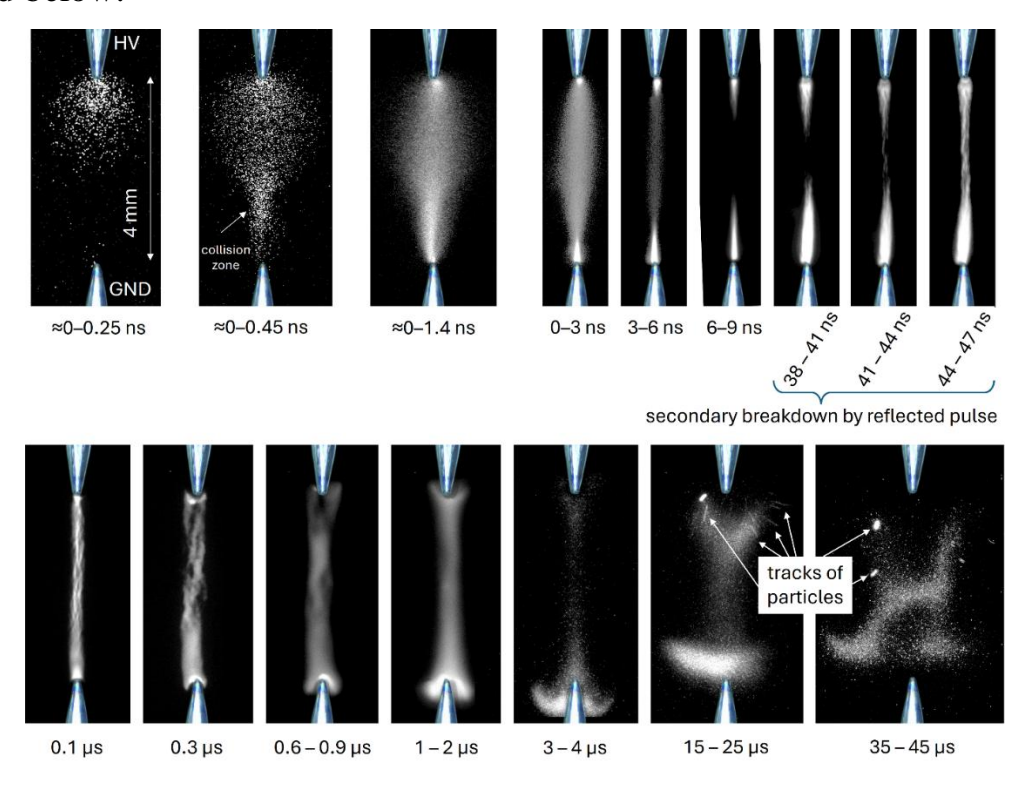


Fig. 3. Time-resolved images of the discharge plasma glow between two needle electrodes. Air, 760 Torr. Maximum energy reserve in HV pulse. HV – high-voltage electrode, GND –opposite electrode shunted through a 75-Ohm resistor.

Increasing the pulse energy (fig. 2b) results in a two-stage discharge combustion. The first stage is diffuse, characterized by a violet glow caused by electron transitions of molecular nitrogen, followed by a spark one (second stage), accompanied by broadband white radiation, as well as the glow of vapors of the electrode material and tracks of particles ejected from electrode surface.

Time-resolved images of the discharge plasma glow between needle electrodes for atmospheric-pressure air (760 Torr) and the case of maximum voltage pulse energy, obtained using the four-channel ICCD camera, are shown in fig. 3.

It follows from these images that the breakdown is initiated in the vicinity of a tip of the HV electrode. Due to the small radius of curvature of the electrode, in this region there is a significant local increase in the electric field, reaching values of several MV/cm. This exceeds the threshold field for avalanche ionization in air (about 30 kV/cm at atmospheric pressure), which leads to intense processes of impact ionization and the formation of electron avalanches and the transition of the avalanche into a streamer.

The initial stage is a process of rapid development of a positive streamer (ionization wave) propagating in the direction of the opposite electrode. A characteristic feature is its large (of the order of the gap) diameter and ball-shaped profile near the tip [8, 37]. This is due to the significant radial component of the electric field strength near the needle tip, which promotes the propagation of the ionization front not only along the gap, but also in the radial direction. The positive streamer has a high propagation speed, reaching almost the middle of the gap in ~ 0.25 ns, which corresponds to the average speed of 10⁸–10⁹ cm/s. After this, a negative streamer is formed near the grounded needle. Its transverse dimensions are smaller, which is probably due to the asymmetric distribution of the field in the gap. After no more than 0.1 ns, a collision of the opposite streamers occurs at a distance of approximately 2/3 of the gap length from the HV electrode. This can be judged by the region of enhanced glow observed both in the time-integrated (Fig. 2a) and time-resolved (Fig. 3, time interval 0–0.45 ns) images. The collision of opposite streamers marks a complete breakdown of the gap and discharge ignition stage, accompanied by a sharp voltage

drop and an increase in the current to a value of ≈ 200 A (Fig. 4a). This is how a diffuse high-voltage discharge is formed (Fig. 3c), the active phase of which, as confirmed by waveforms the of voltage, discharge current and radiation intensity (Fig. 4a), lasts about 13 ns.

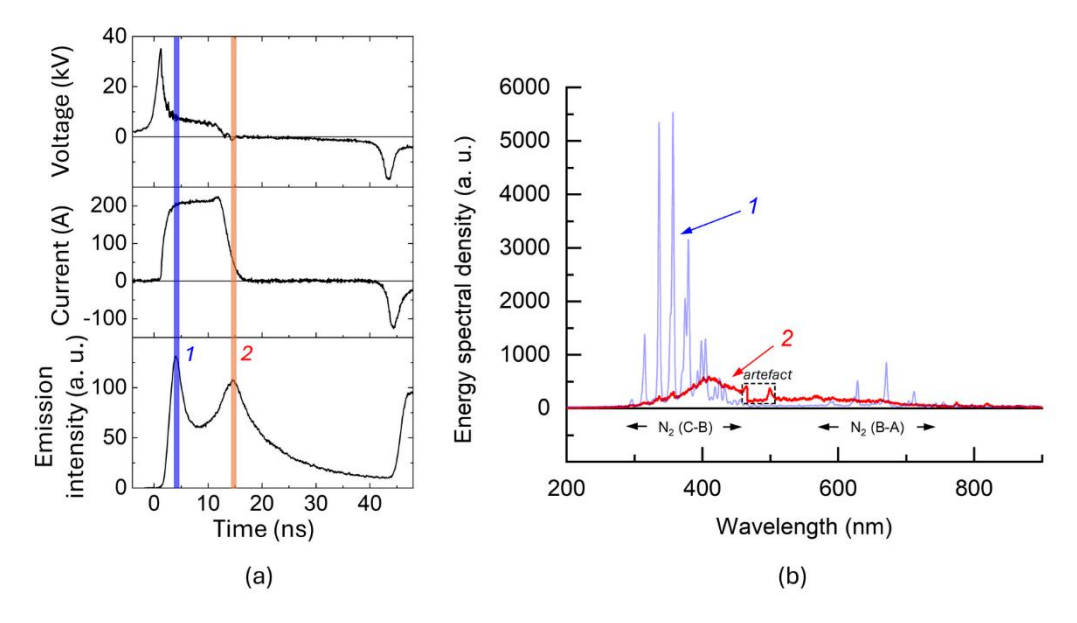


Fig. 4. (a) Waveforms of the voltage across the gap, discharge current, as well as plasma radiation intensity. (b) Plasma emission spectra: 1 – diffuse phase; 2 – spark phase. Needle-needle gap. Air, 760 Torr.

The diffuse discharge implies the formation of a highly non-equilibrium low-temperature plasma, in which the electron temperature ($T_{\rm e}$) significantly exceeds that of heavy particles – gas temperature $T_{\rm g}$. For example, typical values of $T_{\rm e}$ can be 1–3 eV, while $T_{\rm g}$ remains close to room one (0.03 eV). This circumstance is convincingly indicated by the spectral distribution of the radiation energy in Fig. 4b. It is represented mainly by the bands of the first (1⁺) and second (2⁺) positive systems of molecular nitrogen N₂ (range 300–500 nm), as well as the first (1⁻) negative system of the molecular nitrogen ion N₂⁺ (Fig. 4b, I). These spectral systems are indicators of intense ionization and excitation of nitrogen molecules and ions by direct electron impact, which is typical for plasma with a high $T_{\rm e}$ value, but low $T_{\rm g}$.

During the next ~10 ns, a gradual fading of the diffuse glow is observed. At the same time, there is an increase in the brightness of the glow near the tips of both needle electrodes, as well as the formation of separate, brighter and thinner channels in the discharge volume. This is due to the relatively slow, compared to the streamer stage,

development of filaments – narrow plasma channels with an increased current density and concentration of charged particles. The fading of the diffuse glow, in turn, is explained by a rapid decrease in the concentration of excited nitrogen molecules, mainly due to collisional quenching by nitrogen molecules in the ground state.

Using the streak camera equipped with the spectrometer, the emission spectrum of the filaments (Fig. 4b, 2) was obtained. It can be seen that it consists of a broadband continuum with a maximum spectral energy distribution in the wavelength region of 400 nm. This continuum can be associated with strong rapid heating of the gas [38].

The counter filaments do not have time to completely form a spark channel and close the gap during the first current pulse (Fig. 3, time interval 6–9 ns). However, when the voltage pulse reflected from the generator after the first arrival at the gap returns and causes a repeated breakdown (approximately ~ 38 ns after the first one), the filaments merge and a full-fledged spark channel is formed (Fig. 3, time interval 38–47 ns).

It is curious that during the almost 30 ns while the voltage pulse travels to the generator, is reflected from it and returns to the gap, the filament plasma did not recombine completely and retained sufficient conductivity for current to flow. This indicates the existence of long-lived excited states, e.g., metastable nitrogen states such as $N_2(A^3\Sigma_u^+)$. They can serve as an energy reservoir and maintain a residual electron concentration even in the absence of a strong external electric field. Thermal effects such as local heating of the gas inside the filaments, which can prevent rapid recombination, may also play a role. It is also evident that the spark channel at this stage is represented by a set of several microchannels rather than a single continuous channel. This complex structure is preserved during further evolution of the plasma channel under the influence of gas-dynamic processes (such as channel expansion due to gas heating, formation of shock waves), which determine its final shape.

In addition to the rapid breakdown stage and spark channel formation, the later stages of discharge evolution, occurring after the main current pulse has fallen, are of significant interest. On time scales of hundreds of nanoseconds after the spark channel formation, the plasma channel begins to expand actively. This expansion is caused by

a sharp increase in temperature and, as a consequence, gas pressure inside the channel due to intense Joule heating in the spark phase. The expansion occurs at a supersonic speed, generating a shock wave that propagates in the surrounding, undisturbed gas. This process leads to the formation of a cylindrically symmetric low-density region.

It is noteworthy that the own plasma glow continues to be recorded for tens of microseconds after the active discharge phase has ended. This long-lived afterglow allows the complex dynamics of gas-dynamic processes in the gap between the needle electrodes to be visualized. The nature of this afterglow is complex and includes the recombination of electrons and ions, radiation from long-lived metastable states of atoms and molecules (e.g., $N_2(A^3\Sigma_u^+)$), which can accumulate energy and transfer it to other states.

Fig. 5 demonstrates the spatial distribution along the axis of the discharge gap of the ratio $R_{_{391/394}}$ of the peak intensities of the bands of the first negative (1⁻) and second positive (2⁺) systems of the molecular ion N₂⁺ and the nitrogen molecule N₂ and the corresponding electric field strength E, calculated from $R_{391/394}$ according to formula (1).

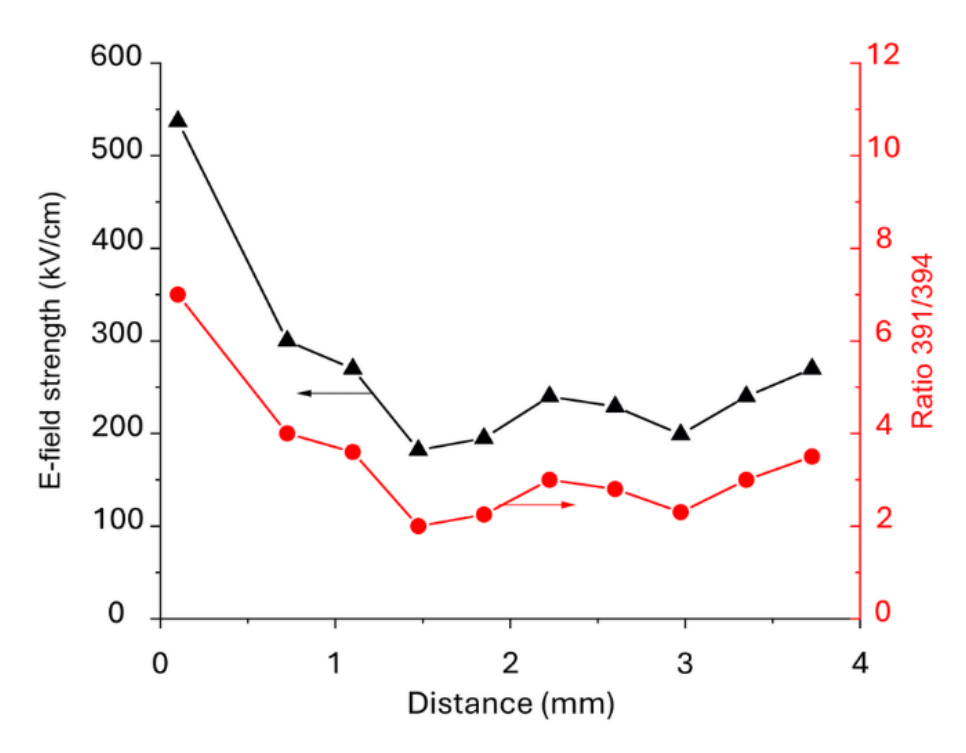


Fig. 5. Spatial distribution along the axis of the discharge gap of the ratio $R_{_{391/394}}$ of the peak intensities of the bands of the first negative (1⁻) and second positive (2⁺) systems of the molecular ion N_2^+ and the nitrogen molecule N_2 , as well as the electric field strength E calculated from $R_{_{391/394}}$.

The spatial distribution of the electric field strength E is important for the analysis of the development of counter streamers. Since under the conditions of the streamer stage of the discharge the direct electron impact is the dominant channel of excitation of nitrogen molecules and their ions, the intensity ratio $R_{391/394}$ directly correlates with the electron energy distribution function and in turn directly depends on the reduced electric field strength E/N. These data allow us to draw conclusions about the dynamics of streamer development. The maximum E is observed near the HV tip (anode). This is explained by the high charge density on the sharp edge of the electrode, where the radius of curvature is minimal, which leads to a significant increase in the field. It is here that the initial ionization and formation of a positive streamer occurs. As the positive streamer develops and propagates in the interelectrode gap, its diameter increases. At the same time, E inside the streamer body decreases. This is due to the fact that the streamer, being conductive, screens the external field, and the main voltage drop occurs at its head, where a strong intrinsic field is created due to the volume charge. With some time delay, the negative streamer starts towards the positive streamer. The streamers meet and collide at approximately 2/3 of the distance from the anode. In this zone, a measurable and noticeable increase in the electric field intensity occurs. This is explained by the vector superposition of the fields of volumetric charges of the heads of positive and negative streamers. The obtained data on the spatial distribution of the electric field and the dynamics of streamers are important for the development of theoretical models of streamers.

Conclusion

In the work, various aspects of the high-voltage nanosecond discharge in the gap between two needle electrodes filled with atmospheric-pressure air were studied. It was revealed that the discharge development goes through two main stages: diffuse and spark. The diffuse stage is characterized by a quasi-uniform plasma glow, in which the bands of the second positive system of molecular nitrogen dominate. The presence of this stage is due to the development of large-diameter opposite streamers propagating at the average speed of 10^8 – 10^9 cm/s. A collision of opposite streamers at the distance

of $\sim 2/3$ of the gap length was experimentally observed, which was accompanied by an increase in both the glow intensity and the electric field strength. The spark stage of the discharge is caused by the development of opposite filaments from the electrodes. The rate of filament propagation is more than an order of magnitude lower than that of streamer. The filament emission is characterized by a broadband continuum with a maximum distribution in the 400 nm region, which may indicate a high gas temperature. The spark channel formed by the filament closure has a multichannel structure, which indicates the complex dynamics of ionization processes.

Funding: The studies were performed in the framework of the State Task for IHCE SB RAS, project # FWRM-2021-0014.

References

- 1. Babich L.P. High-Energy Phenomena in Electric Discharges in Dense Gases. Futurepast. 2003. 358 p.
- Bourdon A., Bonaventura Z., Celestin S. Influence of the pre-ionization background and simulation of the optical emission of a streamer discharge in preheated air at atmospheric pressure between two point electrodes // Plasma Sources Science and Technology. 2010. V. 19. № 3. P. 034012. https://doi.org/10.1088/0963-0252/19/3/034012
- Chen S. et al. Nanosecond repetitively pulsed discharges in N2–O2 mixtures: inception cloud and streamer emergence // Journal of Physics D: Applied Physics.
 2015. V. 48. № 17. P. 175201. https://doi.org/10.1088/0022-3727/48/17/175201
- 4. Tarasenko V.F. (ed.) Runaway Electrons Preionized Diffuse Discharges. Nova Science Publishers, Inc. 2016.

- 5. Tardiveau P. et al. Sub-nanosecond time resolved light emission study for diffuse discharges in air under steep high voltage pulses // Plasma Sources Science and Technology. 2016. V. 25. № 5. P. 054005. https://doi.org/10.1088/0963-0252/25/5/054005
- Aleksandrov N.L. et al. High-voltage pico-and nanosecond discharge development in gaseous and liquid media // Zhurnal Prikladnoi Spektroskopii (Journal of Applied Spectroscopy). – 2016. – V. 83. – № 6-16. – P. 658–659.
- 7. Babaeva N.Y. et al. Development of nanosecond discharges in atmospheric pressure air: two competing mechanisms of precursor electrons production // Journal of Physics D: Applied Physics. − 2018. − V. 51. − № 43. − P. 434002. https://doi.org/10.1088/1361-6463/aada74
- 8. Sorokin D.A. et al. Features of streamer formation in a sharply non-uniform electric field // Journal of Applied Physics. 2019. V. 125. P. 143301. https://doi.org/10.1063/1.5067294
- 9. Bourdon A. et al. Study of the electric field in a diffuse nanosecond positive ionization wave generated in a pin-to-plane geometry in atmospheric pressure air // Journal of Physics D: Applied Physics. − 2020. − V. 54. − № 7. − P. 075204. https://doi.org/10.1088/1361-6463/abbc3a
- 10. Trenkin A.A. et al. Dynamics of Structure of Pulsed Discharge in Nitrogen and Argon at Different Pressures in a "Pin to Plane" Gap // Technical Physics. 2024.
 V. 69. № 2. P. 431-436. https://doi.org/10.21883/jtf.2022.09.52925.58-22
- 11. Huiskamp T. Nanosecond pulsed streamer discharges: Part I: Generation, source-plasma interaction and energy-efficiency optimization // Plasma Sources Science and Technology. 2020. V. 29. № 2. P. 023002.
- 12. Wang D., Namihira T. Nanosecond pulsed streamer discharges: Part II. Physics, discharge characterization and plasma processing // Plasma Sources Science and Technology. − 2020. − v. 29. − № 2. − P. 023001. https://doi.org/10.1088/1361-6595/ab5bf6

- 13. Luo Y. et al. Numerical simulation of surface charge accumulation under negative discharge of different humidities and pressures // Physics of Plasmas. 2025.
 V. 32. № 2. P. 023901. https://doi.org/10.1063/5.0241349
- 14. Tarasenko V. et al. Properties of diffuse and volume discharges that are important for their applications // High Voltage. − 2025. − V. 10. − № 1. − P. 126-136. https://doi.org/10.1049/hve2.12507
- 15. Baksht E. Kh. et al. Point-like pulse-periodic UV radiation source with a short pulse duration // Quantum Electronics. 2012. V. 42. № 2. P. 153–156. https://doi.org/10.1070/QE2012v042n02ABEH014795
- 16. Cha M.S., Snoeckx R. Plasma technology–Preparing for the electrified future // Frontiers in Mechanical Engineering. 2022. V. 8. P. 903379. https://doi.org/10.3389/fmech.2022.903379
- 17. Adamovich I. et al. The 2022 Plasma Roadmap: low temperature plasma science and technology // Journal of Physics D: Applied Physics. 2022. V. 55. № 37. P. 373001.
- 18. Pawelek D.B. et al. Design of a nanosecond high voltage surface discharge switch // 2007 IEEE 34th International Conference on Plasma Science (ICOPS). IEEE, 2007. P. 348–348. https://doi.org/10.1109/PPPS.2007.4345654
- 19. Chaparro J.E. et al. Breakdown delay times for subnanosecond gas discharges at pressures below one atmosphere // IEEE Transactions on Plasma Science. 2008.
 V. 36. № 5. P. 2505–2510. https://doi.org/10.1109/TPS.2008.2004365
- 20. Beloplotov D., Sorokin D., Tarasenko V. High-voltage nanosecond discharge as a means of fast energy switching // Energies. 2021. V. 14. № 24. P. 8449. https://doi.org/10.3390/en14248449
- 21. Becker K.H., Kogelschatz U., Schoenbach K.H., Barker R.J. (eds.). Non-equilibrium air plasmas at atmospheric pressure. CRC press, 2004. 700 p. https://doi.org/10.1201/9781482269123
- 22. Starikovskiy A. Pulsed nanosecond discharge development in liquids with various dielectric permittivity constants // Plasma sources science and Technology. 2013.
 V. 22. № 1. P. 012001. https://doi.org/10.1088/0963-0252/22/1/012001

- 23. Prukner V. et al. Demonstration of dynamics of nanosecond discharge in liquid water using four-channel time-resolved ICCD microscopy. Plasma. 2021. V. 4. P. 183–200. https://doi.org/10.3390/plasma4010011
- 24. Hoder T. et al. Barrier discharges in CO₂–optical emission spectra analysis and E/N determination from intensity ratio // Plasma Sources Science and Technology.

 2025. V. 34. № 5. P. 055008. https://doi.org/10.1088/1361-6595/adc7d7
- 25. Lu X. et al. Reactive species in non-equilibrium atmospheric-pressure plasmas: Generation, transport, and biological effects // Physics Reports. 2016. V. 630. P. 1-84. https://doi.org/10.1016/j.physrep.2016.03.003
- 26. Komuro A. A review of streamer discharge-induced plasma chemistry at atmospheric pressure: Key mechanisms and future perspectives // Journal of Electrostatics. 2025. P. 104087. https://doi.org/10.1016/j.elstat.2025.104087
- 27. Weltmann K.-D. et al. The future for plasma science and technology // Plasma Processes and Polymers. 2019.– V. 16. № 1. P. 1800118. https://doi.org/10.1002/ppap.201800118
- 28. Šimek M., Homola T. Plasma-assisted agriculture: history, presence, and prospects—a review // The European Physical Journal D. 2021. V. 75. P. 1–31. https://doi.org/10.1140/epid/s10053-021-00206-4
- 29. S. Duarte, Panariello B.H.D. Comprehensive biomedical applications of low temperature plasmas // Archives of Biochemistry and Biophysics. 2020. V. 693. P. 108560. https://doi.org/10.1016/j.abb.2020.108560
- 30. Minesi N.Q. et al. Plasma-assisted combustion with nanosecond discharges. I: Discharge effects characterization in the burnt gases of a lean flame // Plasma Sources Science and Technology. − 2022. − V. 31. − № 4. − P. 045029. https://doi.org/10.1088/1361-6595/ac5cd4
- 31. Mouele E.S.M. et al. A critical review on ozone and co-species, generation and reaction mechanisms in plasma induced by dielectric barrier discharge technologies for wastewater remediation // Journal of Environmental Chemical Engineering. 2021. V. 9. №. 5. P. 105758

- 32. Parkevich E.V. et al. Streamer formation processes trigger intense x-ray and high-frequency radio emissions in a high-voltage discharge // Physical Review E. 2022.

 V. 105. № 5. P. L053201. https://doi.org/10.1103/PhysRevE.105.L053201
- 33. Sorokin D.A., Beloplotov D.V. Development of Nanosecond Discharge in an Inhomogeneous Electric Field in Water Medium // Bulletin of the Russian Academy of Sciences: Physics. 2024. V. 88. № 4. P. 656-663. https://doi.org/10.1134/S1062873823706268
- 34. Efanov V.M., et al. Ultra-Wideband, Short Pulse Electromagnetics 9. Springer, 2010. p. 301. https://doi.org/10.1007/978-0-387-77845-7_35
- 35. Paris P. et al. Intensity ratio of spectral bands of nitrogen as a measure of electric field strength in plasmas // Journal of Physics D: Applied Physics. 2005. V. 38. № 21. P. 3894–3899. https://doi.org/10.1088/0022-3727/38/21/010
- 36. Hoder T. et al. Radially and temporally resolved electric field of positive streamers in air and modelling of the induced plasma chemistry // Plasma Sources Science and Technology. 2016. V. 25. № 4. P. 045021. https://doi.org/10.1088/0963-0252/25/4/045021
- 37. Beloplotov D.V. et al. Measurement of the dynamic displacement current as a new method of study of the dynamics of formation of a streamer at a breakdown of gases at a high pressure // JETP Letters. 2018. V. 107. P. 606-611. https://doi.org/10.1134/S0021364018100065
- 38. Popov N.A. Fast gas heating in a nitrogen–oxygen discharge plasma: I. Kinetic mechanism // Journal of Physics D: Applied Physics. 2011. V. 44. № 28. P. 285201. https://doi.org/10.1088/0022-3727/44/28/285201
- 39. Dumitrache C. et al. Hydrodynamic regimes induced by nanosecond pulsed discharges in air: mechanism of vorticity generation // Journal of Physics D: Applied Physics. 2019. V. 52. № 36. P. 364001. https://doi.org/10.1088/1361-6463/ab28f9

- 40. Tholin F., Bourdon A. Simulation of the hydrodynamic expansion following a nanosecond pulsed spark discharge in air at atmospheric pressure // Journal of Physics D: Applied Physics. 2013. V. 46. № 36. P. 365205. https://doi.org/10.1088/0022-3727/46/36/365205
- 41. Roger E. et al. Origin of the recirculation flow pattern induced by nanosecond discharges and criterion for its development // Journal of Physics D: Applied Physics. 2025. V. 58. № 14. P. 145203. https://doi.org/10.1088/1361-6463/adb1f0

For citation:

Beloplotov D.V., Zaitsev B., Sorokin D.A. Features of the formation of a high-voltage nanosecond discharge in a "point-to-point" gap filled with atmospheric pressure air // Journal of Radio Electronics. − 2025. − № 11. https://doi.org/10.30898/1684-1719.2025.11.21